Int J Adv Manuf Technol (2015) 78:1329–1336
DOI 10.1007/s00170-014-6752-0

ORIGINAL ARTICLE

Wear characteristics and wear control method of PVD-coated carbide tool in turning Inconel 718

ZhaoPeng Hao · YiHang Fan · JieQiong Lin · ZhiXin Yu

Received: 9 September 2014 / Accepted: 19 December 2014 / Published online: 7 January 2015

Abstract As nickel-based alloy Inconel 718 has poor thermal conductivity and serious work hardening, it is classified as a difficult-to-cut material. The tool wear is very serious. In this paper, PVD-coated carbide tools were employed to cut Inconel 718. Firstly, tool wear morphology and tool wear mechanism were studied. The results show that tool wear characteristic changed with cutting speeds. There was an optimum cutting speed at which oxides serving as boundary lubrication layer formed. These oxides can reduce the friction coefficient of the tool-chip contact surface and inhibit tool wear. Secondly, according to the wear mechanism analysis, tool flank wear model was established in the light of wear delamination theory. The optimum cutting temperature was proposed, and it was calculated using the established model. At the optimum cutting temperature, tool wear can reach the minimum value. At last, verification experiments for the optimum cutting temperature were carried out. For a pair of tool-workpiece, the minimal tool wear can be obtained by optimizing cutting conditions so as to make the cutting temperature reach the optimum value. This provides a good method for tool wear control. It also provides a theoretical basis and effective means for a reasonable choice of cutting parameters.

Keywords Inconel 718 · PVD-coated carbide tool · Tool wear characteristics · Optimum cutting temperature · Tool wear control

Nomenclature

G	Shear modulus
b	Burgers vector
ν	Poisson's ratio
σ_f	Stress needed to overcome by dislocation motion
P	Normal load received by tool wear surface
s_0	Critical slip distance when the debris formed
h	Tool flank wear thickness
K, C	Constant
dl	Unit cutting length
Φ	The diameter of workpiece material
VB	Tool flank wear width
α_o	Tool relief angle
γ_o	Tool rake angle
λ_s	Edge inclination
κ_r	Cutting edge angle
θ	Cutting temperature
v_c	Cutting speed
f	Feed rate
a_p	Cutting depth

Z. Hao · Y. Fan (✉) · J. Lin · Z. Yu
School of Mechatronic Engineering, ChangChun University of Technology, ChangChun 130012, China
e-mail: fyh1911@126.com

1 Introduction

Nickel-based alloy is widely used for the production of structural parts such as aerospace engine and turbine disk and blades, due to its superior performance such as high-temperature strength and resistance to oxidation and corrosion. However, because of its poor thermal conductivity, high chemical activity, and work hardening, the cutting tool wears seriously. Inconel 718 is one kind of the most used nickel-based alloy. It is classified as "difficult-to-cut materials" and more and more researchers have paid attention to tool wear mechanism in the process of cutting Inconel 718.

The choice of cutting tool is an important factor in machining nickel-based alloys. Regarding tool material selection, many researchers analyzed the cutting performance of cemented carbide tool (uncoated and coated) and ceramic and cubic boron nitride (CBN) cutting tools. In general, in

machining nickel-based alloy, when the cutting speed ranges up to 30 m/min, uncoated inserts were usually used, and when up to 100 m/min, the cemented carbide tools should properly coated [1].

Ceramic and CBN tools have superior hot hardness and can be used at speeds around an order of magnitude higher than the coated carbide cutting tools; especially a high cutting speed can be achieved when using the whisker-reinforced ceramics [2]. CBN cutting tools improve the cutting performance and give considerable increment in cutting speed when machining nickel-based alloys because of their notch wear resistance; however, it should be considered their elevated cost [3].

Despite the advances in tool materials for cutting nickel-based alloys, coated cemented carbides are still competitive and widely used in the industry [4]. Furthermore, comparative analyses for different coating materials were also studied. The results showed that physical vapor deposition (PVD)-TiAlN-coated tool is the best choice for cutting Inconel 718 due to its excellent mechanical properties under the conditions of high-temperature friction [5, 6].

Tool wear mechanisms involved in sliding friction occur at the contact interface between tool, chip, and machined surface [7]. Under some conditions, the softer oxides generating in the cutting process acted as a boundary lubrication layer, which made the chemical wear and adhesive wear reach equilibrium. They can inhibit the formation of built up edge (BUE) and high-temperature adhesion and reduce their negative effects on surface quality effectively [8].

Regarding the carbide tool wear mechanism, the cutting force and cutting temperature are very high in the process of cutting Inconel 718. The serious adhesion and notch wear are the key factors leading to tool failure [1]. Bhatt believed that abrasive and adhesive wear were the most dominant wear mechanisms, controlling the deterioration and final failure of the WC tools in finish turning of Inconel 718 [9]. Devillez put forward that the formation and falling off of unstable BUE near cutting edge under high temperature and pressure is one important cause of tool wear [6]. Due to high work hardening of the Ni alloy, significant notch wear was observed. The side cutting edge angle k_γ has strong effects on tool wear evolution. Increasing k_γ diminishes the cutting aggressiveness for the tool [4].

Through observing the tool wear morphology, Hao et al. studied the wear mechanism of PVD-coated (TiAlN) tool in dry machining Inconel 718. They came to a conclusion that the main reason which causes cutting tool wear was that the tool materials fall off from the tool substrate in the form of wear debris. In addition, element diffusion between tool and workpiece and oxidation reaction all accelerate the formation and the peeling of the wear debris [10].

Díaz-Álvarez et al. applied a 3D numerical model based on finite element (FE) to the simulation of dry turning of Inconel 718. The main wear modes experimentally identified (chipping, notching, built up edge (BUE)) were related to variables predicted using the numerical model, such as temperature and plastic strain at the chip. Good correlation between experiments and numerical results was observed in their studies. They also found that the side cutting edge k_γ had strong influence on wear performance [11].

In view of the serious tool wear in machining Inconel 718, many researchers tried to improve the performance of cutting tool by reducing cutting force and cutting temperature. Virginia et al. studied the mechanism involved in the improvement of Inconel 718 machinability by laser-assisted machining (LAM). They found that LAM can reduce the work hardening which led to a lower notch wear. The risk of sudden failure of tool was reduced, which resulted in a controllable tool life [12]. Hsu employed the ultrasonic vibration cutting tool and the workpiece of high-temperature heating to cut Inconel 718. This method improved surface quality, reduced cutting force, and increased tool life [13]. Fan et al. studied tool wear mechanism in machining Inconel 718 under water vapor + air cooling lubrication cutting conditions. Compared with the dry cutting, under water vapor + air cooling lubrication cutting conditions, tool wear mechanism mainly relates the weak oxidation wear of W and Co elements instead of serious adhesion and abrasive wear, thereby enhancing the tool life [14].

These new methods mentioned above can effectively improve the service life of the cutting tool, to some extent. However, the high cost, inconvenient installation, and operation of the auxiliary equipment limited its wide application. Furthermore, in order to reach green manufacturing, more and more researchers have paid considerable attentions to dry machining by eliminating cutting fluids [15].

In the present study, based on the analysis of tool wear mechanism, the tool flank wear model was established in the light of wear delamination theory. The optimum cutting temperature was proposed, and it was calculated using the established model. At the optimum cutting temperature, tool wear can reach the minimum value. Therefore, for a pair of tool-workpiece, the minimal tool wear can be achieved by optimizing cutting conditions so as to make the cutting temperature reach the optimum value. This provides a good method for tool wear control, and the present method is easy to implement and use in the factory.

2 Materials and experiment process

The workpiece used in this study was an Inconel 718 bar of a diameter of 100 mm. Mechanical properties and chemical components of Inconel 718 are shown in Table 1. The tool material and their geometric parameters are shown in Table 2.

Charge-coupled device (CCD) observation system and scanning electron microscopy (SEM) with energy dispersive X-ray spectrometer (EDS) were employed to observe tool

Table 1 Chemical components and mechanical performance of Inconel 718

Material	Chemical composition (W_t), %										Mechanical performance of Inconel 718					
	Ni	Cr	Nb	Mo	Ti	C	Si	Mn	B	Fe	Yield σ0.2 (MPa)	Tensile σ_b (MPa)	Toughness a_k (J/cm^2)	Shrinkage ψ (%)	Elongation δ_5 (%)	Density ρ (kg/m^3)
Inconel 718	51.75	17	5.15	2.93	1.07	0.042	0.21	0.03	0.006	Last	1260	1430	40	40	24	8280

wear morphology. X-ray photoelectron spectroscopy (XPS) was used to analyze the chemical reaction and existing state of the element.

The average cutting temperature was measured with the natural thermocouples. The cutting force signals in three directions were recorded with the cutting force measurement system, which was composed of Kistler9257A three-dynamometer, data acquisition card, and 5007 charge amplifier.

In machining process, the cutting speed v_c has more great effects on tool wear than feed rate and cutting depth. The experiments were carried out at the cutting speed 20, 32, and 45 m/min. The cutting depth and feed rate kept constant (f= 0.1 mm/r, a_p=1 mm).

3 Results and discussion

3.1 Tool wear characteristics

When cutting speed v_c=20 m/min, the micrographs by SEM of tool surface is shown in Fig. 1 According to Fig. 1a, a lot of adhesion materials adhered to tool surface. The frequent generation and falling off of the adhesion materials led to the fluctuation of cutting force, and then caused tool chipping (Fig. 1b).

It also leads to a crack between tool coating and tool substrate and then the PVD film is cut by workpiece material and then peels off with the cutting process going on, as shown in Fig. 2.

Micrographs by SEM of tool wear surface when v_c=32 m/min is shown in Fig. 3. The tool surface was relatively smooth, and a small amount of wear debris formed in the worn surface. Moreover, a uniform gray film layer adhered to wear surface. X-ray photoelectron spectroscopy (XPS) was used to analyze the chemical components and existing state of elements. The results are shown in Fig. 4.

According to Fig. 4, the electron binding energy of elements reflects the presence state of the elements. Electron binding energies 708.2, 709.4, and 710.8 eV represent that of Fe_3O_4, FeO, and Fe_2O_3, respectively, which shows that the following reaction occurred.

$$3Fe + 2O_2 = Fe_3O_4$$
$$2Fe + O_2 = 2FeO$$
$$4Fe + 3O_2 = 2Fe_2O_3$$

The electron binding energies 576.8 and 576.3 eV represents that of Cr_2O_3 and CrO_2, respectively, which shows that the following reaction occurred.

$$4Cr + 3O_2 = 2Cr_2O_3$$
$$Cr + O_2 = CrO_2$$

The generated soft oxides served as a boundary lubrication layer which can effectively inhibit the adhesion between tool and workpiece and reduce the friction coefficient, and then protect cutting tool. According to the XPS analysis results, there are not peaks indicating the binding energy of Co (780.2 eV) and W (35 eV) elements, which shows that oxidation reaction did not occur for the elements of tool material.

Figure 5 illustrates tool wear morphology at v_c=45 m/min. Tool wear surface showed to be uneven. The gray film layer was broken seriously and a lot of wear debris formed. The XPS analysis results of tool wear surface are shown in Fig. 6.

According to Fig. 6, the oxidation has occurred in tool substrate material. The electron binding energies 779.9, 780.2, and 780.4 eV represents that of Co_2O_3, Co_3O_4, and CoO, respectively. The electron binding energies 32.8, 35, and 35.8 eV represents that of WO_3, $CoWO_3$, and WO_2, respectively. The electron binding energy 31.4 eV represents that of elemental W. This shows that the following reaction occurred.

$$4\ Co + 3\ O_2 = 2\ Co_2O_3$$
$$3\ Co + 2\ O_2 = Co_3O_4$$
$$2\ Co + O_2 = 2\ CoO$$
$$WC + Co + 3O_2 = CoWO_4 + CO_2\uparrow$$
$$WC + 1/2\ O_2 = W + CO\uparrow$$
$$WC + O_2 = W + CO_2\uparrow$$
$$WC + O_2 = WO_2 + C$$
$$WC + 3/2O_2 = WO_2 + CO\uparrow$$
$$WC + 3/2\ O_2 = WO_3 + C$$
$$WC + 2O_2 = WO_3 + CO\uparrow$$
$$WC + 2O_2 = WO_2 + CO_2\uparrow$$
$$WC + 5/2O_2 = WO_3 + CO_2\uparrow$$

Table 2 Information of workpiece and tool

	Material	Geometric parameters
Workpiece	Inconel 718	Φ100×500 mm (bar)
Cutting tool	PVD-TiAlN-coated carbide	γ_0=6°, α_0=7°, λ_s=−4°, κ_r=45°

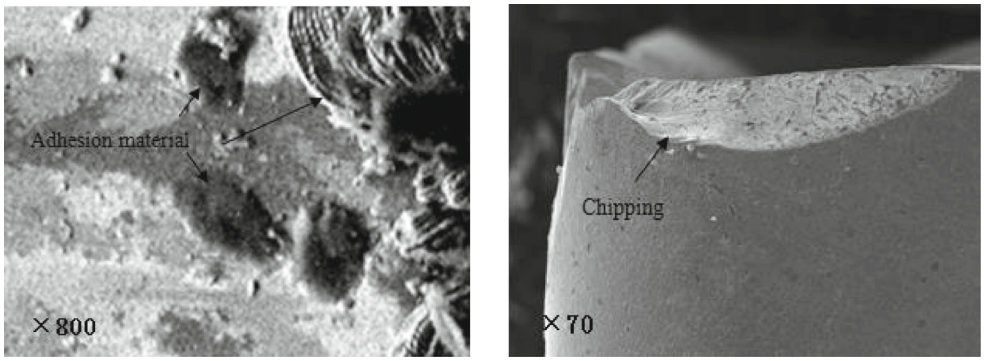

(a) Adhesion (b)Tool chipping

Fig. 1 Micrographs by SEM of tool wear surface when v_c=20 m/min. **a** Adhesion. **b** Tool chipping

Because of the oxidation reaction of W and Co, the oxides Co_2O_3, Co_3O_4, WO_3, $CoWO_3$, WO_2, etc. weakened the adhesion force of Co element and reduced the tool strength. The wear debris increased in tool surface and it intensified tool wear.

3.2 Tool wear control method

According to the above analysis of tool wear characteristics, the adhesion and surface fatigue caused by chip flowing led to the falling off of flakes of wear debris from the tool substrate, which was the principal wear mechanism for cutting tool. The tool wear characteristics are the main features of the delamination theory of sliding wear. Therefore, it is reasonable to use the delamination theory to establish tool wear model in machining Inconel 718.

In the light of the delamination theory, the thickness of wear debris can be expressed as

$$h = \frac{\mathrm{Gb}}{4\pi(1-\nu)\sigma_f}\mathrm{Ps}_0 \tag{1}$$

In Eq. (1), σ_f is the stress needed to overcome by dislocation motion. However, in the light of the mechanical properties of carbide tool material, σ_f can be treated as the fracture strength of carbide material.

When unit cutting length is dl, the tool flank wear thickness can be expressed as

$$h = \frac{KPdl}{\sigma_f} \tag{2}$$

where K=Gb/(4π(1−ν)). It is a constant.

Figure 7 shows the geometry relationship between tool flank wear thickness h and wear width VB.

According to the Fig. 7,

$$d\mathrm{VB} = h\cdot(\mathrm{ctg}\alpha_0 - \tan\gamma_0) \tag{3}$$

$$d\mathrm{VB} = K\frac{P\cdot dl}{\sigma_f}\cdot(\mathrm{ctg}\alpha_0 - \tan\gamma_0) \tag{4}$$

Integrating both sides, this equation was rewritten as

$$\int d\mathrm{VB} = \int K\frac{P\cdot \mathrm{dl}}{\sigma_f}\cdot(\mathrm{ctg}\alpha_0 - \tan\gamma_0) \tag{5}$$

$$\int d\mathrm{VB} = K\frac{P}{\sigma_f}\cdot(\mathrm{ctg}\alpha_0 - \tan\gamma_0)\int dl \tag{6}$$

Fig. 2 Tool coating cracking

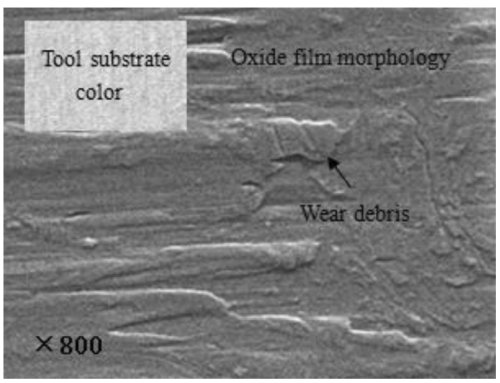

Fig. 3 Micrographs by SEM of tool wear surface when v_c=32 m/min

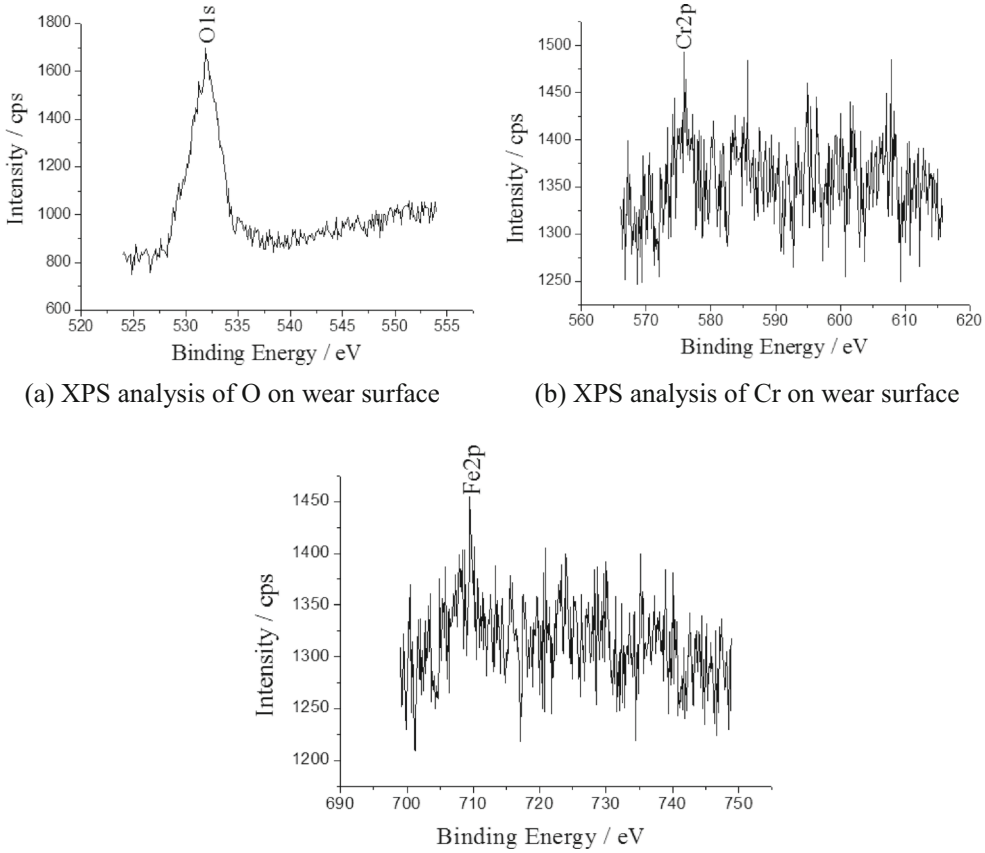

Fig. 4 XPS analysis results of tool wear surface (v_c=32 m/min). **a** XPS analysis of O on wear surface. **b** XPS analysis of Cr on wear surface. **c** XPS analysis of Fe on wear surface

(a) XPS analysis of O on wear surface

(b) XPS analysis of Cr on wear surface

(c) XPS analysis of Fe on wear surface

The flank wear width VB can be expressed as

$$\mathrm{VB} = K\frac{Pl}{\sigma_f}\cdot(\mathrm{ctg}\alpha_0 - \tan\gamma_0) + C \tag{7}$$

When l=0, VB=0, we can get C=0. The Eq. (7) can be rewritten as

$$\mathrm{VB} = K\frac{Pl}{\sigma_f}\cdot(\mathrm{ctg}\alpha_0 - \tan\gamma_0) \tag{8}$$

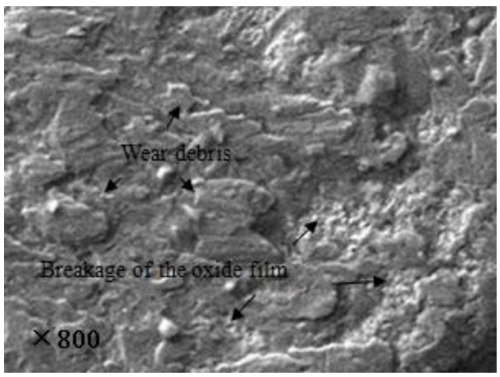

Fig. 5 Tool wear morphology when v_c=45 m/min

From the Eq. (8), for the given cutting tool and cutting length, we can get that

$$\mathrm{VB} \propto \frac{P}{\sigma_f} \tag{9}$$

In cutting process, for a given friction pair of tool-workpiece, cutting temperature is one of the important factors affecting the chemical reaction of element and the strength ratio of tool-workpiece. The cutting temperature is controllable by changing cutting conditions. Therefore, there exists an optimum cutting temperature at which tool wear can get the minimum value [10]. Furthermore, cutting temperature is the principal factor that influences tool strength and cutting process. Therefore, the normal load P and the fracture strength of tool material σ_f can be written as a function of cutting temperature:

$$P = f_1(\theta); \sigma_f = f_2(\theta) \tag{10}$$

and then,

$$\mathrm{VB} \propto \frac{f_1(\theta)}{f_2(\theta)} \tag{11}$$

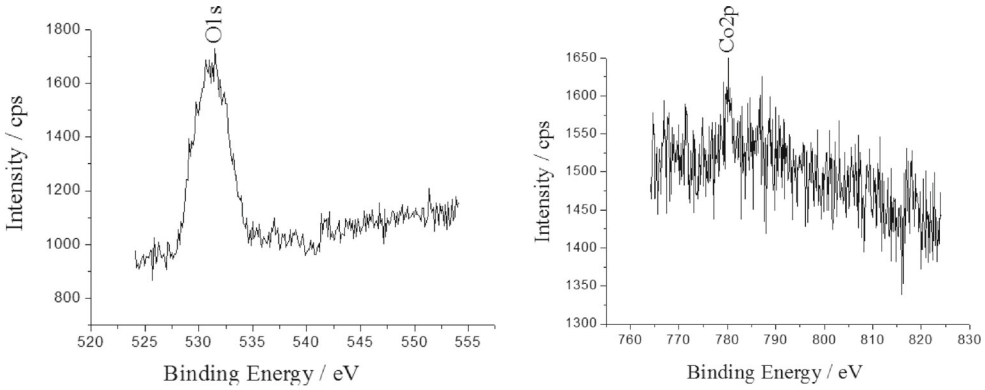

Fig. 6 XPS analysis results of tool wear surface (v_c=45 m/min). **a** XPS analysis of O on wear surface. **b** XPS analysis of Co on wear surface. **c** XPS analysis of W on wear surface

(a) XPS analysis of O on wear surface

(b) XPS analysis of Co on wear surface

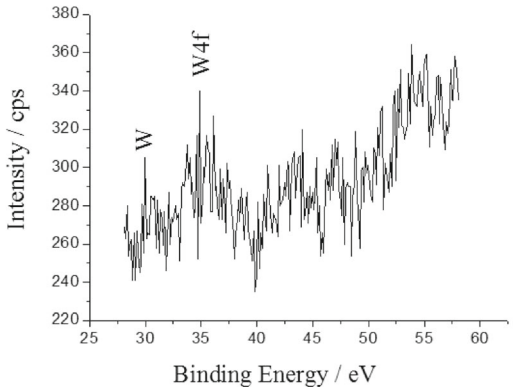

(c) XPS analysis of W on wear surface

Because the optimum cutting temperature is a constant and cutting speed has more great effects on cutting temperature than feed rate, the experiments were conducted with constant feed rate to obtain the relationship between P and θ.

$$P = f_1(\theta) = 3307.3\theta^{-0.4} \tag{12}$$

Figure 8 illustrates the variation of fracture strength σ_f with cutting temperature θ [16].

The function relation of σ_f and θ was obtained according to Fig. 7.

$$\sigma_f = f_2(\theta) = 371 + \frac{1766}{1 + e^{\frac{\theta - 788}{54}}} \tag{13}$$

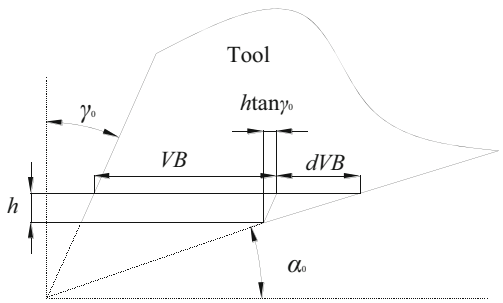

Fig. 7 Geometry relationship between h and VB

In order to make the VB get the minimal value, letting $d\mathrm{VB}/d\theta$=0, thereby the optimum temperature was calculated, which was equal to 619 °C.

3.3 Experimental verification

The verification experiments were conducted with different combinations of cutting parameters under the same cutting length. The tool flank wear width was measured, and the results are shown in Fig. 9.

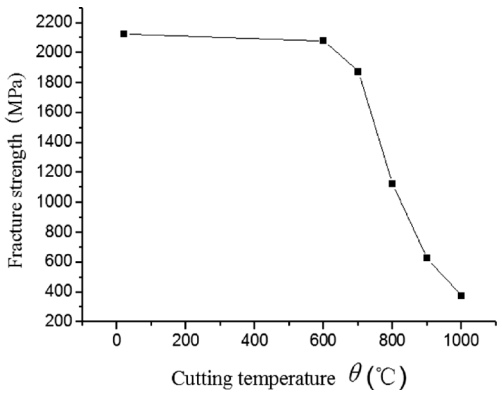

Fig. 8 σ_f–θ curve

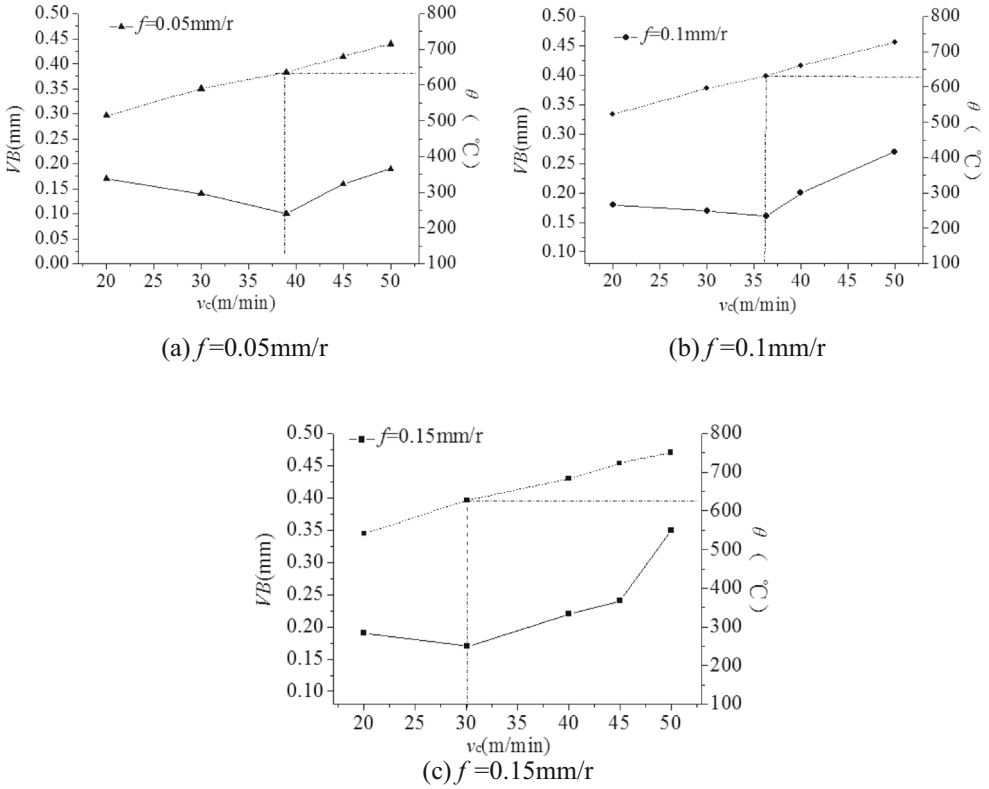

Fig. 9 Results of tool flank wear width in verification experiments. **a** f=0.05 mm/r, **b** f=0.1 mm/r, **c** f=0.15 mm/r

According to Fig. 9, for the given cutting parameters in cutting Inconel 718, when tool wear reached the minimal, the cutting temperature was near the optimum cutting temperature. This means that for a pair of tool-workpiece, the minimal tool wear can be achieved by optimizing cutting conditions so as to make the cutting temperature reach the optimum value. This provides a good method for tool wear control.

4 Conclusions

In this paper, the tool wear characteristics and wear control method based on optimum cutting temperature were studied in turning Inconel 718 employing PVD-coated carbide tools. The conclusions can be drawn as

(1) Tool wear mechanism varied with cutting speed. At a low cutting speed (v_c=20 m/min), the serious adhesion led to crack between tool coating and tool substrate and tool chipping. When cutting speed v_c=32 m/min, the new generated oxide film adhered to wear surface. The oxide film served as a boundary lubrication layer, which reduced the friction coefficient of the tool-chip contact surface and inhibit tool wear. With cutting speed increased further (v_c=45 m/min), the lubricant film was broken seriously and a lot of wear debris generated. The oxidation reaction occurred in tool substrate material. Because of the oxidation reaction of W and Co, the oxides Co_2O_3, Co_3O_4, WO_3, $CoWO_3$, WO_2, etc. weakened the adhesion force of Co element and reduced the tool strength. The wear debris increased in tool surface and it intensified tool wear.

(2) The optimum cutting temperature was proposed and it was calculated using the established flank model. At the optimum cutting temperature, tool wear can reach the minimum value. For a pair of tool-workpiece, the minimal tool wear can be achieved by optimizing cutting conditions so as to make the cutting temperature reach the optimum value. This provides a good method for tool wear control.

Acknowledgments This work is supported by Key Scientific and Technological Project of Jilin Province—"Research on the turning device and key technology in high efficiency and high quality cutting nickel-based alloy."

References

1. Olovsj S, Nyborg L (2012) Influence of microstructure on wear behavior of uncoated WC tools in turning of Alloy718 and Waspaloy. Wear 282–283:12–21. doi:10.1016/j.wear.2012.01.004
2. Altin A, Nalbant M, Taskesen A (2007) The effects of cutting speed on tool wear and tool life when machining Inconel 718 with ceramic tools. Mater Des 28:2518–2522. doi:10.1016/j.matdes.2006.09.004

3. Costes JP, Guillet Y, Poulachon G, Dessoly M (2007) Tool-life and wear mechanisms of CBN tools in machining of Inconel 718. Int J Mach Tools Manuf 47:1081–1087. doi:10.1016/j.ijmachtools.2006.09.031
4. Cantero JL, Díaz-Álvarez J, Miguélez MH, Marín NC (2013) Analysis of tool wear patterns in finishing turning of Inconel 718. Wear 297:885–894. doi:10.1016/j.wear. 2012.11.004
5. Nalbant M, Altin A, Gökkaya H (2007) The effect of coating material and geometry of cutting tool and cutting speed on machinability properties of Inconel 718 super alloys. Mater Des 28:1719–1724. doi:10.1016/j.matdes.2006.03.003
6. Devillez A, Schneider F, Dominiak S, Dudzinski D, Larrouquere D (2007) Cutting forces and wear in dry machining of Inconel 718 with coated carbide tools. Wear 262:931–942. doi:10.1016/j.wear.2006.10.009
7. Fan YH, Hao ZP, Lin JQ, Yu ZX (2014) Material response at tool-chip interface and its effects on tool wear in turning Inconel 718. Mater Manuf Process 29:1446–1452. doi:10.1080/10426914.2014.921701
8. Fan YH, Hao ZP, Zheng ML, Sun FL, Yang SC (2013) Study of surface quality in machining nickel-based alloy Inconel 718. Int J Adv Manuf Technol 69:2659–2667. doi:10.1007/s00170-013-5225-1
9. Bhatt A, Attia H, Vargas R, Thomson V (2010) Wear mechanisms of WC coated and uncoated tools in finish turning of Inconel 718. Tribol Int 43:1113–1121. doi:10.1016/j.triboint.2009.12.053
10. Hao ZP, Gao D, Fan Y, Han RD (2011) New observations on tool wear mechanism in dry machining Inconel 718. Int J Mach Tools Manuf 51:973–979. doi:10.1016/j.ijmachtools.2011.08.018
11. Díaz-Álvarez J, Cantero JL, Miguélez H, Soldani X (2014) Numerical analysis of thermomechanical phenomena influencing tool wear in finishing turning of Inconel 718. Int J Mech Sci 82:161–169. doi:10.1016/j.ijmecsci.2014.03.010
12. Virginia GN, Iban A, Oscar G, Josu L (2013) Mechanisms involved in the improvement of Inconel 718 machinability by laser assisted machining (LAM). Int J Mach Tools Manuf 74:9–28. doi:10.1016/j.ijmachtools.2013.06.009
13. Hsu CY, Lin YY, Lee WS, Lo SP (2008) Machining characteristics of Inconel 718 using ultrasonic and high temperature-aided cutting. J Mater Process Technol 198:359–365. doi:10.1016/j.jmatprotec.2007.07.015
14. Fan YH, Hao ZP, Lin JQ, Yu ZX (2014) New observations on tool wear mechanism in machining Inconel 718 under water vapor+air cooling lubrication cutting conditions. J Clean Prod. doi:10.1016/j.jclepro. 2014.11.049
15. Umbrello D (2013) Investigation of surface integrity in dry machining of Inconel 718. Int J Adv Manuf Technol 69:2183–2190. doi:10.1007/s00170-013-5198-0
16. Acchar W, Gomes UU, Kaysser WA, Goring J (1999) Strength degradation of a tungsten carbide-cobalt composite at elevated temperatures. Mater Charact 43:27–32. doi:10.1016/S1044-5803(98)00056-4